Theoretical aspects of pentaquark searches

Adam Szczepaniak (Indiana U.)

Two examples from the past

Pentaquark sightings and kinematic effects

Based in part on collaboration with Dzierba and Meyer

Exchange degeneracy

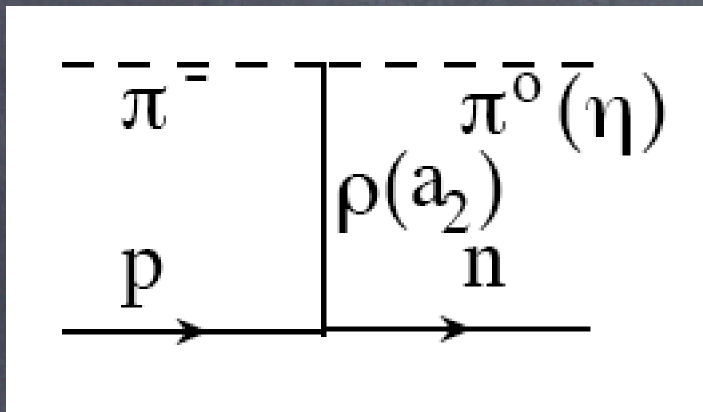

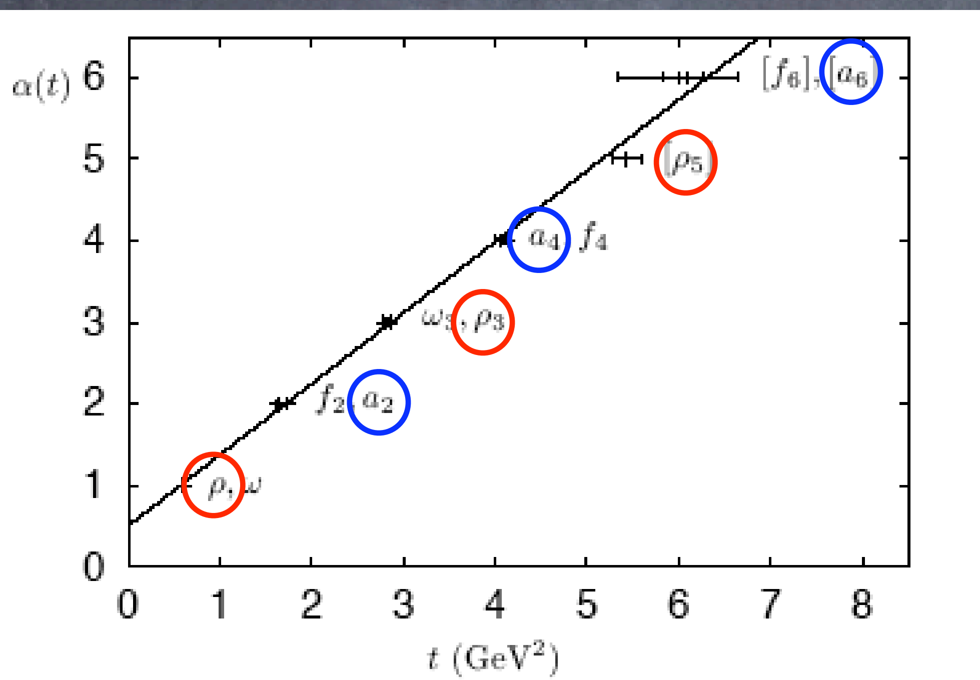

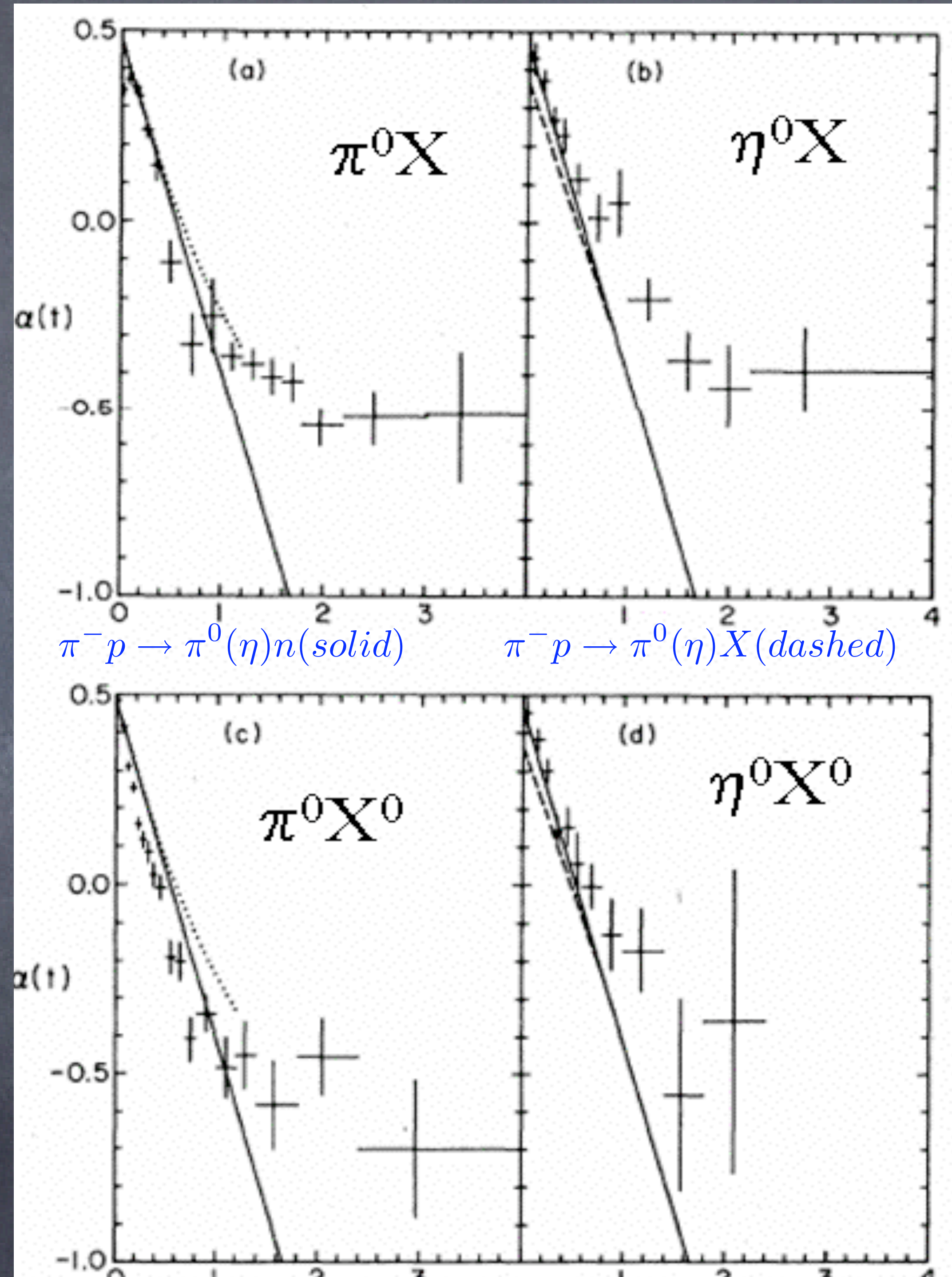

$$\alpha_\rho(t) = \alpha_{a_2}(t) \sim 0.5 + t$$

Strong exchange degeneracy $\gamma_\rho(t) = \gamma_{a_2}(t)$

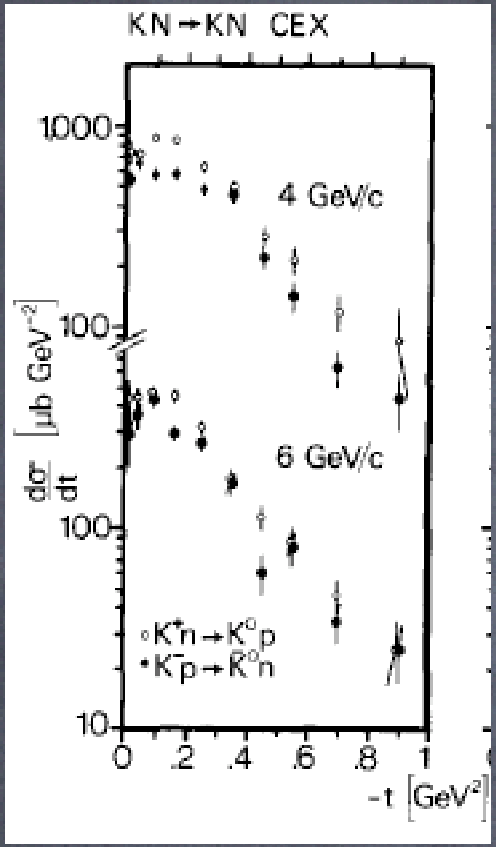

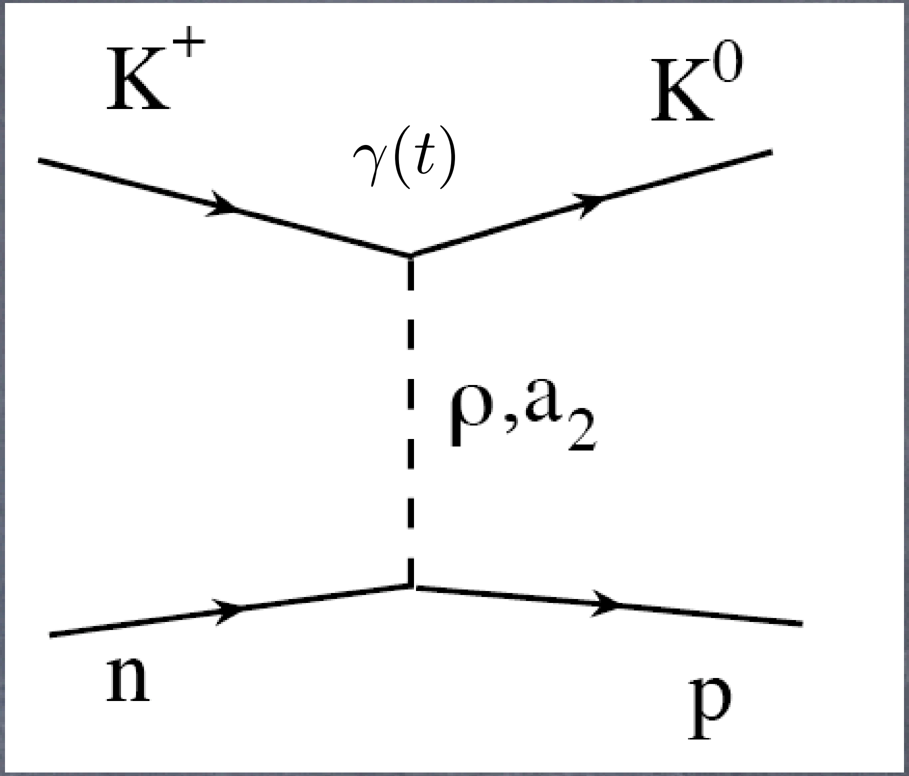

$$A(K^+ n \to K^0 p) = \rho + a_2 = 2\gamma(s/s_0)^\alpha$$ Real !

$$A(K^- p \to \bar{K}^0 n) = \rho - a_2 = -2\gamma(s/s_0)^\alpha e^{-i\pi\alpha}$$

Amplitude at low (resonances) and high (reggions) energy is constrained by analyticity.

Σ_i 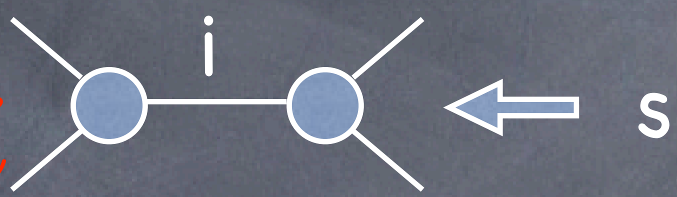

$\sim$ Σ_j 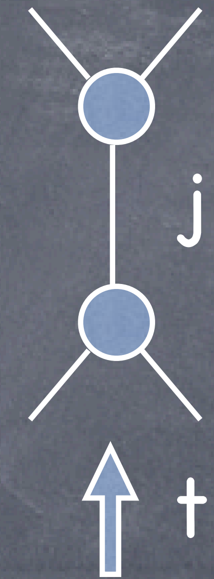

$\sigma \sim$ Im A sizable if there are resonances

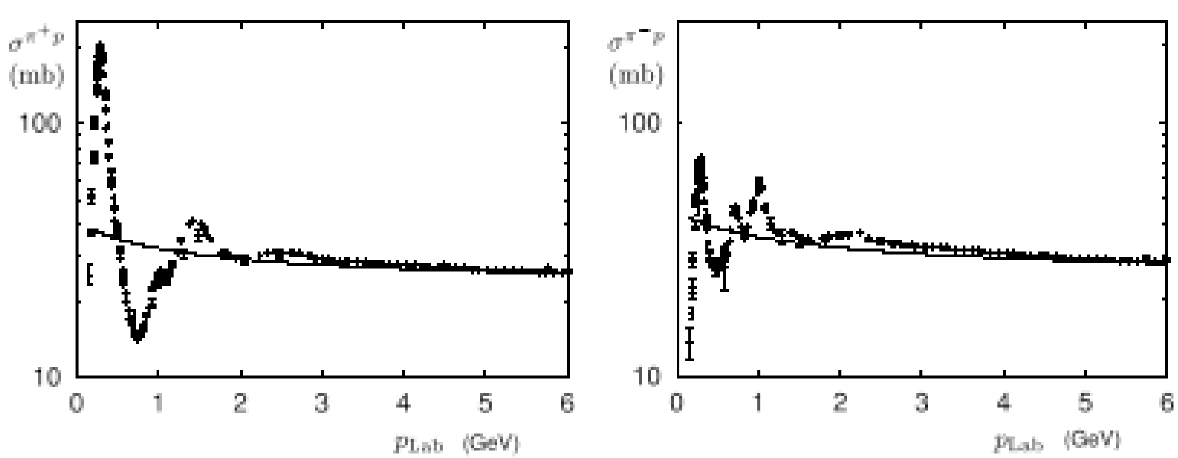

FIG. 6. Total π^+p (left plot) and π^-p (right plot) cross sections as a function of laboratory momentum, p_{Lab}, compared with Regge fits to high energy data. (Adapted from Ref. [18].)

Real CEX K^+n amplitude → No resonances in K^+n

SEARCH FOR THE Z* IN $\pi^- + p \rightarrow K^- + Z^*$ AT 6 AND 8 GeV/c‡

E. W. ANDERSON, E. J. BLESER‡‡, H. R. BLIEDEN, G. B. COLLINS, D. GARELICK
J. MENES and F. TURKOT
Brookhaven National Laboratory, Upton, New York, USA

$$\pi^- + p \rightarrow B^{*-} + p$$
$$\quad\quad \hookrightarrow K^0 + K^-$$
$$\rightarrow B^{*0} + n$$
$$\quad\quad \hookrightarrow K^+ + K^- .$$

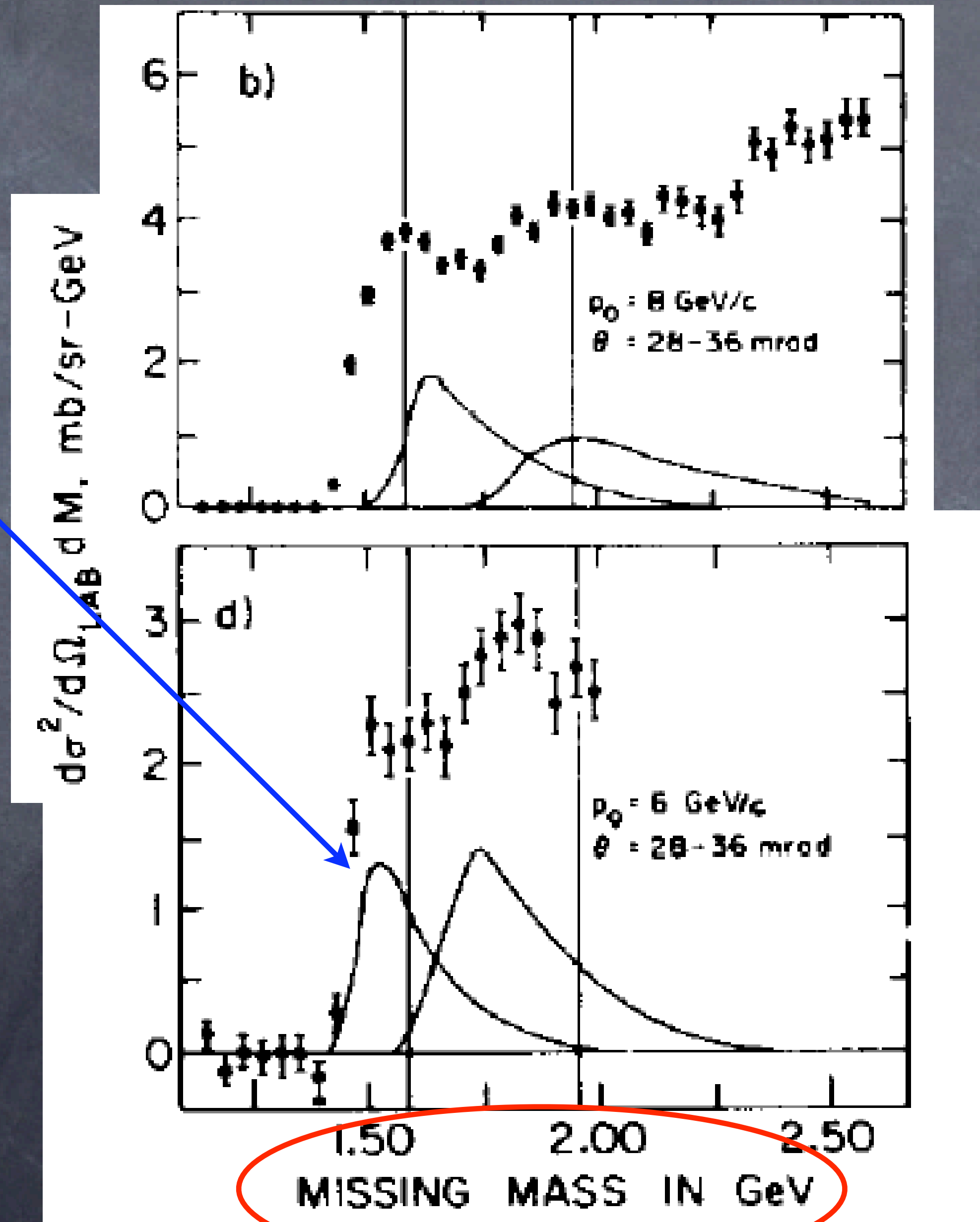

Pentaquark sightings

5q: positive results

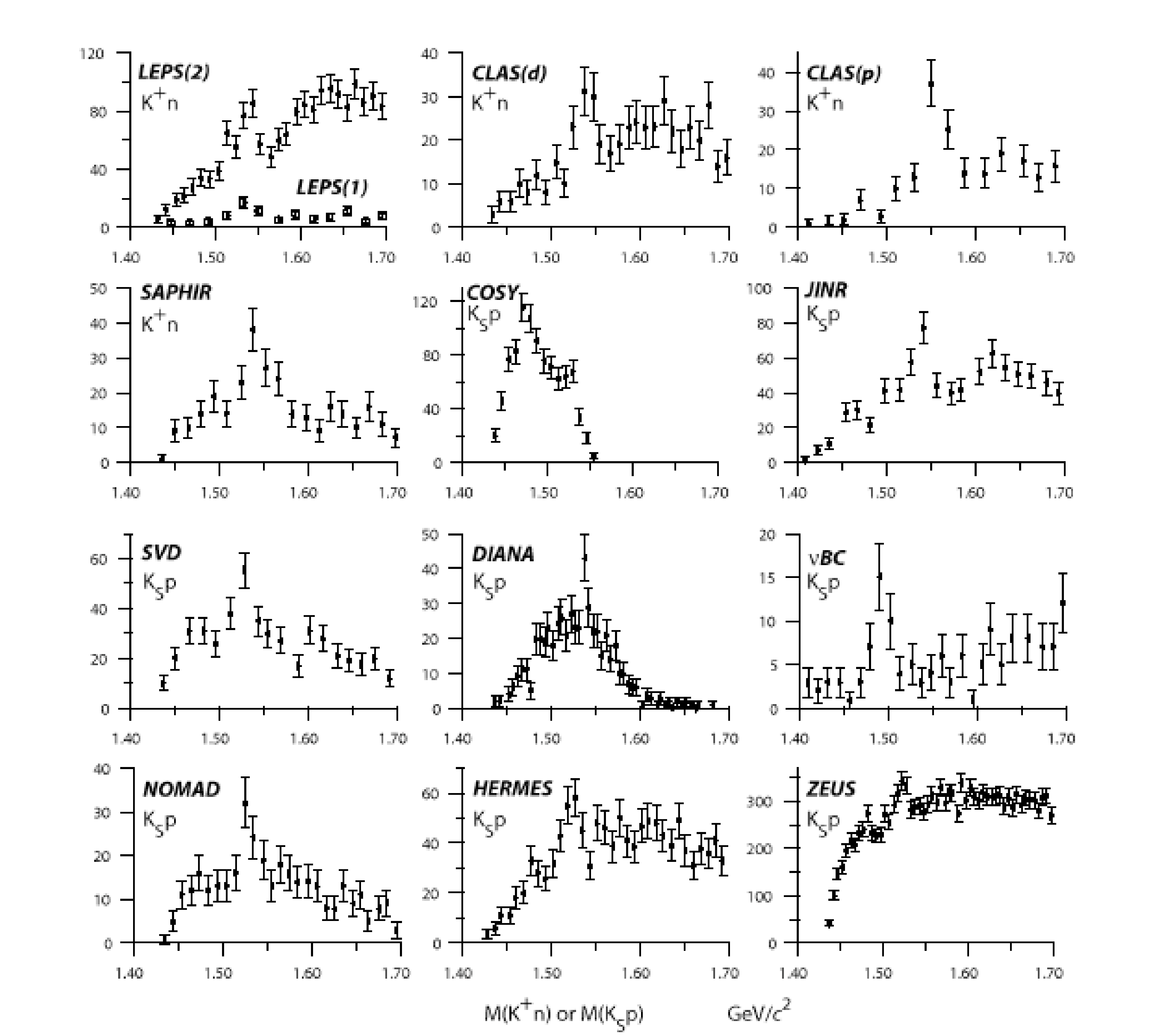

Table 3. A tabulation of statistics for the observations of the θ^+. See text for descriptions of the statistical significance as quoted in the three columns of ratios. The column labeled Published is the significance quoted in the publication.

Experiment	Signal s	Background b	Significance Published	$\frac{s}{\sqrt{b}}$	$\frac{s}{\sqrt{s+b}}$	$\frac{s}{\sqrt{s+2b}}$
LEPS(1) [4]	19	17	4.6	4.6	3.2	2.6
LEPS(2) [5]	56	162		4.4	3.8	2.9
CLAS(d) [6]	43	54	5.2	5.9	4.4	3.5
CLAS(p) [7]	41	35	7.8	6.9	4.7	3.9
SAPHIR [8]	55	56	4.8	7.3	5.2	4.3
COSY [9]	57	95	$4-6$	5.9	4.7	3.7
JINR [10]	88	192	5.5	6.4	5.3	4.1
SVD [11]	35	93	5.6	3.6	3.1	2.4
DIANA [12]	29	44	4.4	4.4	3.4	2.7
νBC [13]	18	9	6.7	6.0	3.5	3.0
NOMAD [14]	33	59	4.3	4.3	3.4	2.7
HERMES [15]	51	150	$4.3-6.2$	4.2	3.6	2.7
ZEUS [16]	230	1080	4.6	7.0	6.4	4.7

5q: negative results

Table 2. Recent negative searches for pentaquark states. For each pentaquark state (P) we indicated with a – that the state was not included in the search while $\Downarrow$ indicates that the state was searched for and not observed and $\Uparrow$ indicates that the state was searched for and observed.

Experiment	Search Reaction	θ^+	Ξ_5	θ_c	Reference
ALEPH	Hadronic Z decays	$\Downarrow$	$\Downarrow$	$\Downarrow$	[19]
BaBar	$e^+e^- \rightarrow \Upsilon(4S)$	$\Downarrow$	$\Downarrow$	–	[20]
BELLE	$KN \rightarrow PX$	$\Downarrow$	–	$\Downarrow$	[21]
BES	$e^+e^- \rightarrow J/\psi(\psi(2S) \rightarrow \theta\bar{\theta}$	$\Downarrow$	–	$\Downarrow$	[22]
CDF	$p\bar{p} \rightarrow PX$	$\Downarrow$	$\Downarrow$	$\Downarrow$	[23]
COMPASS	$\mu^+(^6LiD) \rightarrow PX$	$\Downarrow$	$\Downarrow$	–	[24]
DELPHI	Hadronic Z decays	$\Downarrow$	–	–	[25]
E690	$pp \rightarrow PX$	$\Downarrow$	$\Downarrow$	–	[26]
FOCUS	$\gamma p \rightarrow PX$	$\Downarrow$	$\Downarrow$	$\Downarrow$	[27]
HERA-B	$pA \rightarrow PX$	$\Downarrow$	$\Downarrow$	–	[28]
HyperCP	$(\pi^+, K^+, p)Cu \rightarrow PX$	$\Downarrow$	–	–	[29]
LASS	$K^+p \rightarrow K^+n\pi^+$	$\Downarrow$	–	–	[30]
L3	$\gamma\gamma \rightarrow \theta\bar{\theta}$	$\Downarrow$	–	–	[25, 31]
PHENIX	$AuAu \rightarrow PX$	$\Downarrow$	–	–	[32]
SELEX	$(\pi, p, \Sigma)p \rightarrow PX$	$\Downarrow$	–	–	[33]
SPHINX	$pC(N) \rightarrow \theta^+C(N)$	$\Downarrow$	–	–	[34]
WA89	$\Sigma^-N \rightarrow PX$	–	$\Downarrow$	–	[36]
ZEUS	$ep \rightarrow PX$	$\Uparrow$	$\Downarrow$	$\Downarrow$	[16, 37, 38]

Kinematic reflections in $\gamma n \to K^+ K^- n$

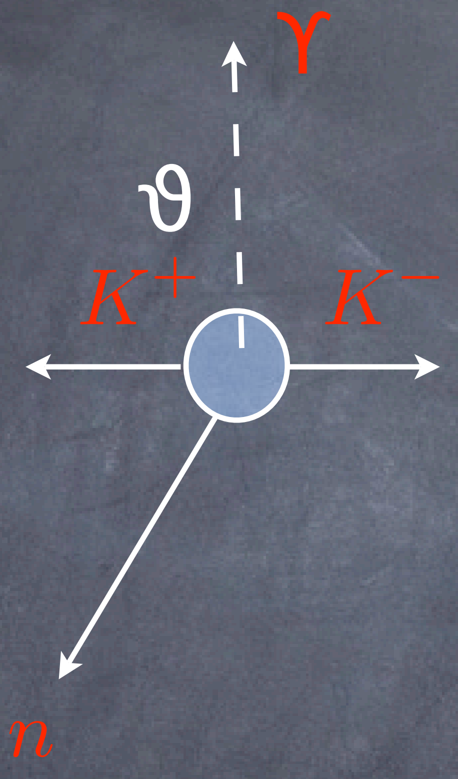

A K^+K^- resonance in its rest frame distributes K's according to its spin ~ $Y_{SM}(\vartheta)$

3-body kinematics $\cos(\vartheta) \sim M_{K+n}$

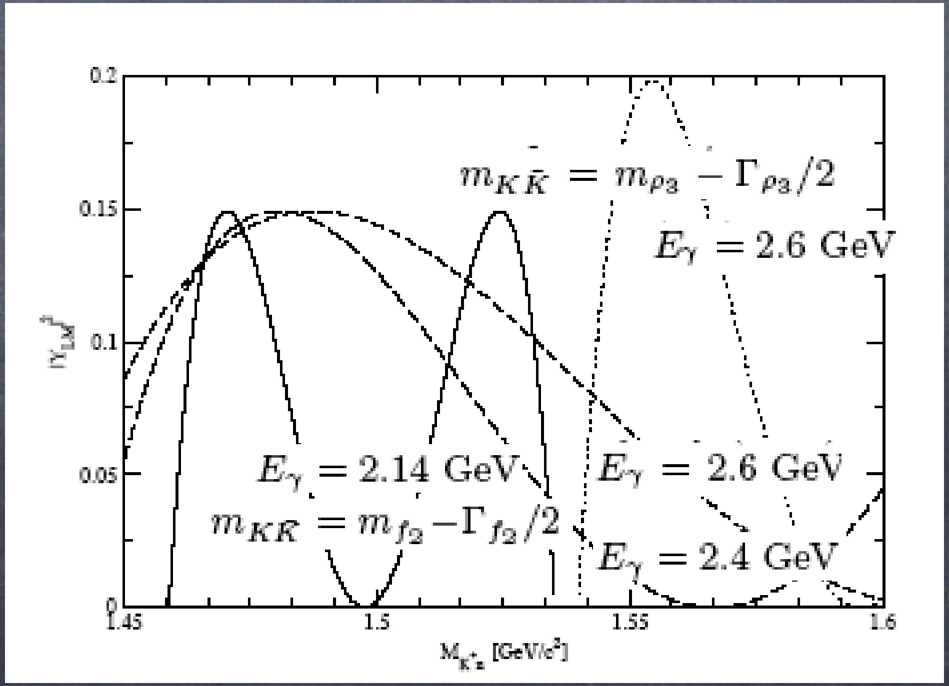

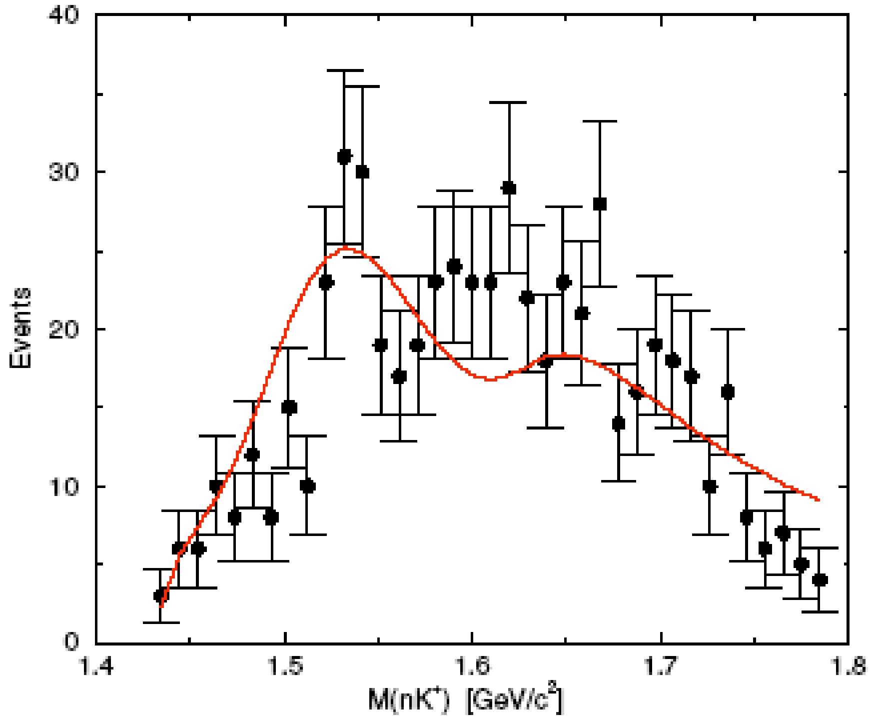

FIG. 3: The calculated (solid line) m_{KN} distribution, as described in the text, compared with the data from [2]

Reaction	Beam energy GeV	Cross Section μb	Ref
$\gamma p \to f_2 p$	2.3-2.6	1.3 ± 0.37	[6]
$\gamma p \to f_2 p$	2.6-3.25	0.39 ± 0.13	[6]
$\gamma p \to f_2 p$	3.25-4.0	0.19 ± 0.06	[6]
$\gamma p \to f_2 p$	4.0-6.3	0.1 ± 0.1	[6]
$\gamma p \to a_2^+ n$	4.2 ± 0.5	1.14 ± 0.43	[7]
$\gamma p \to a_2^+ n$	5.25 ± 0.55	0.85 ± 0.43	[7]
$\gamma p \to a_2^+ n$	7.5 ± 0.7	0.43 ± 0.43	[7]
$\gamma p \to K^+K^- p$	2.8	1.0 ± 0.1	[8]
$\gamma p \to K^+K^- p$	4.7	0.7 ± 0.1	[8]

TABLE I: Photoproduction cross sections for the $f_2(1275)$ and $a_2(1320)$ resonances and the K^+K^- final state.

Physical background has structure >> reduces the statistical significance of the signal

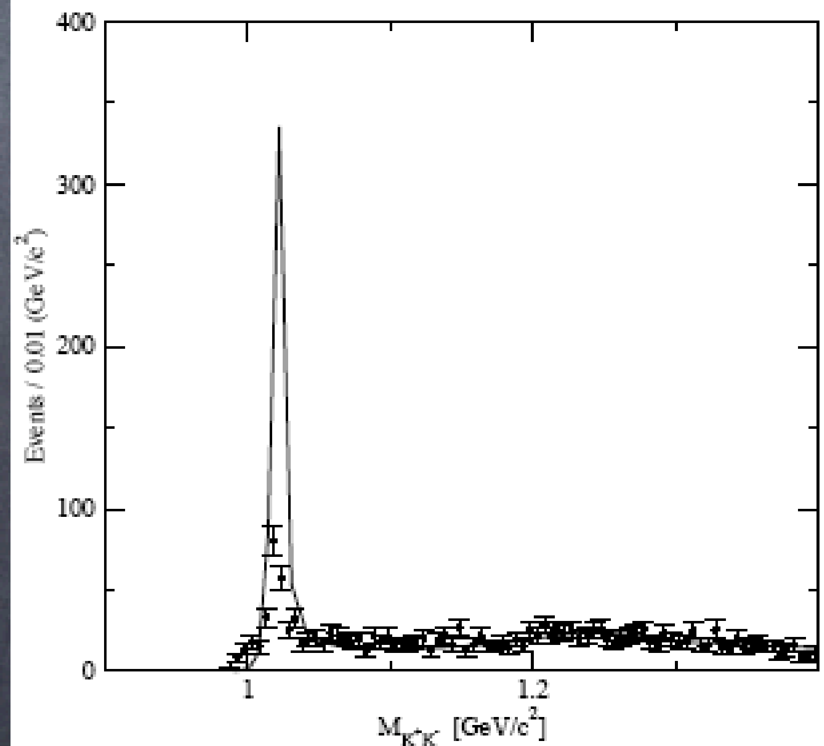

Fake Peaks

Enhancement is broad
- but starting with:

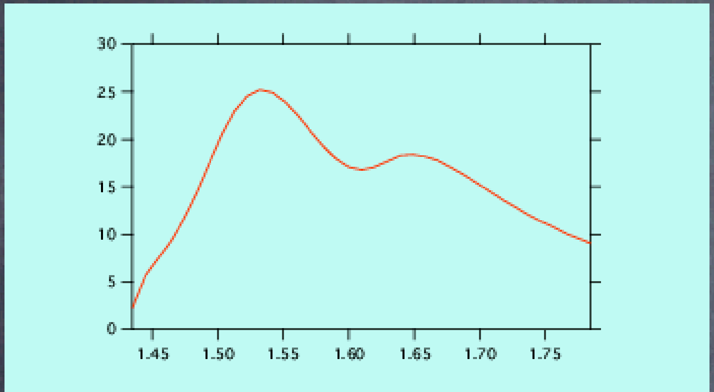

as a parent distribution generate 40 random histograms with 600 events each - 3 of these along with CLAS results appear here

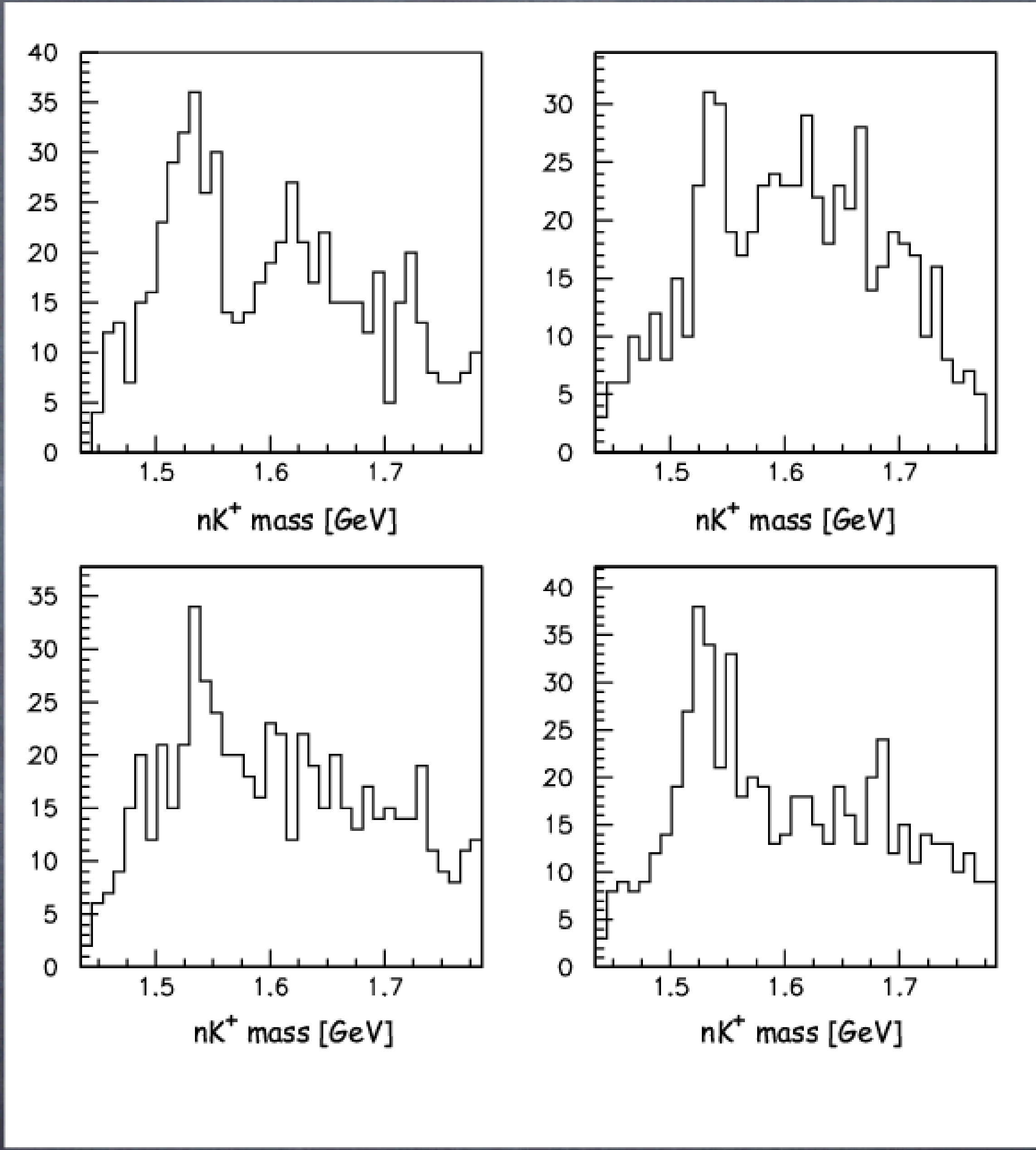

CLAS (proton) $\gamma p \to \pi^+ K^- K^+ n$

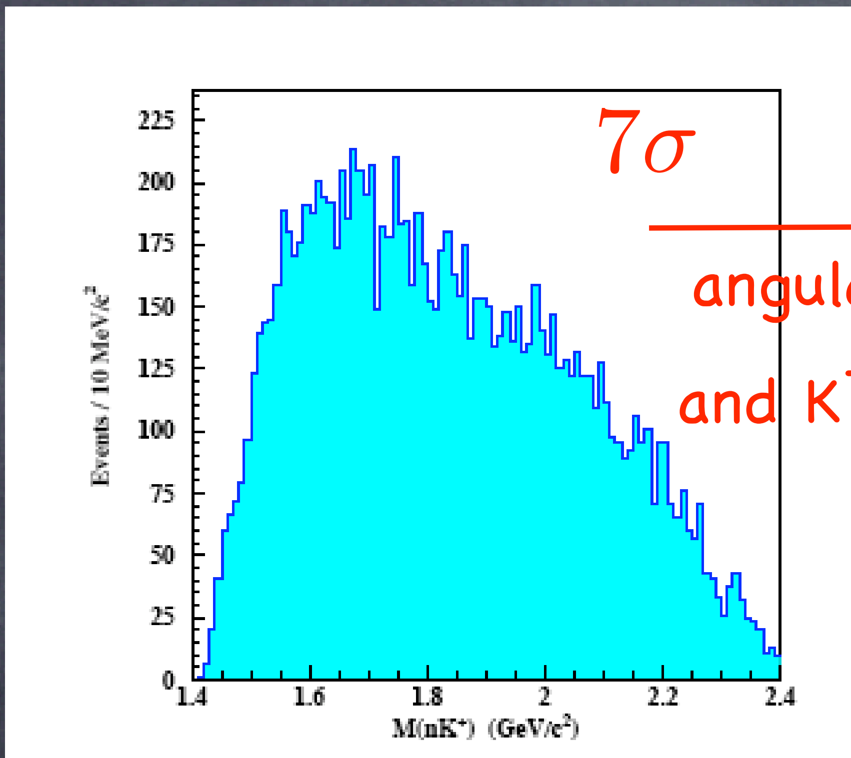

7σ

angular cuts on π^+

and K^+ momenta

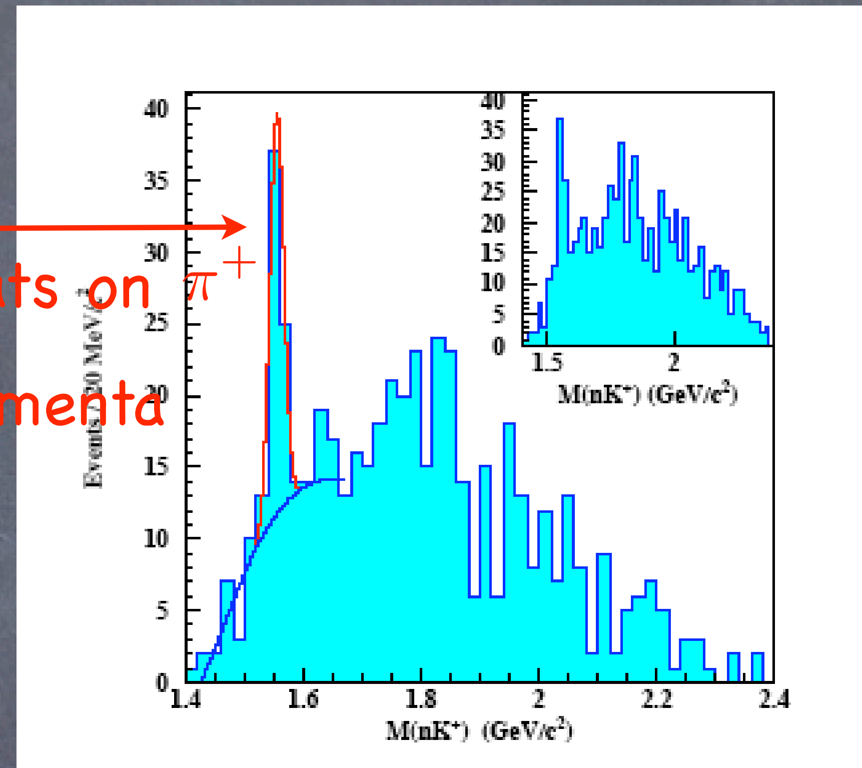

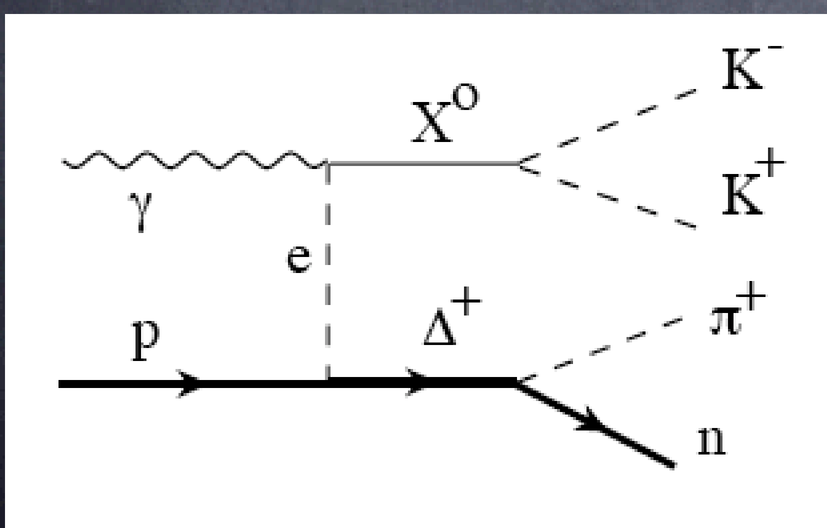

Can generate resonance-like structure in K^+K^-n spectrum and π^+ momentum cut enhances kinematic reflections from decays of K^+K^- resonances

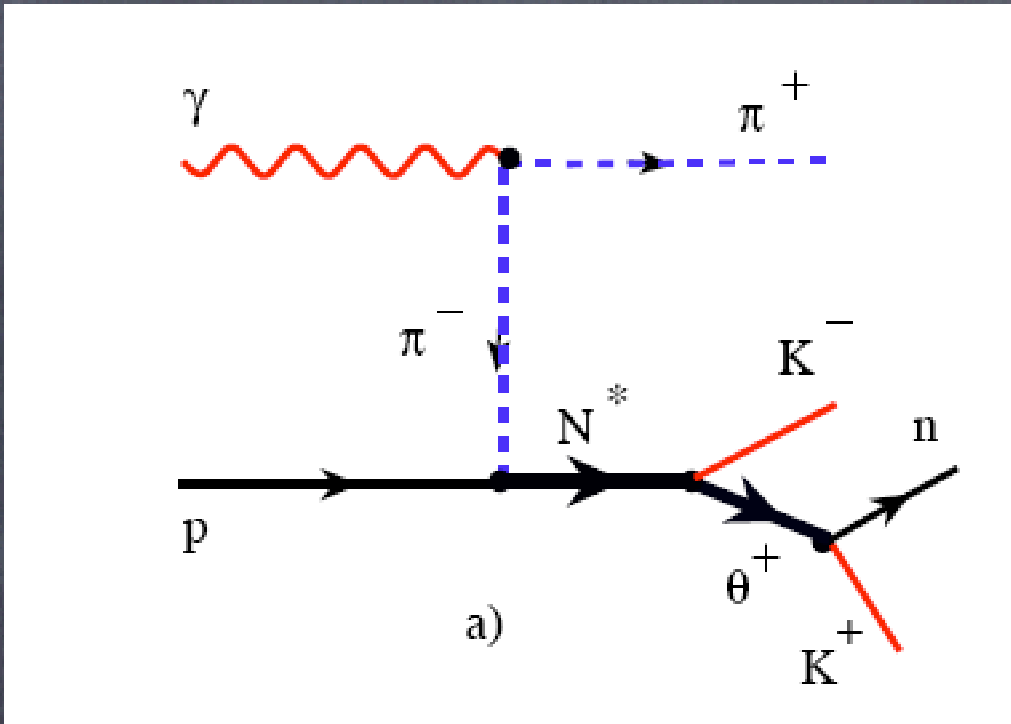

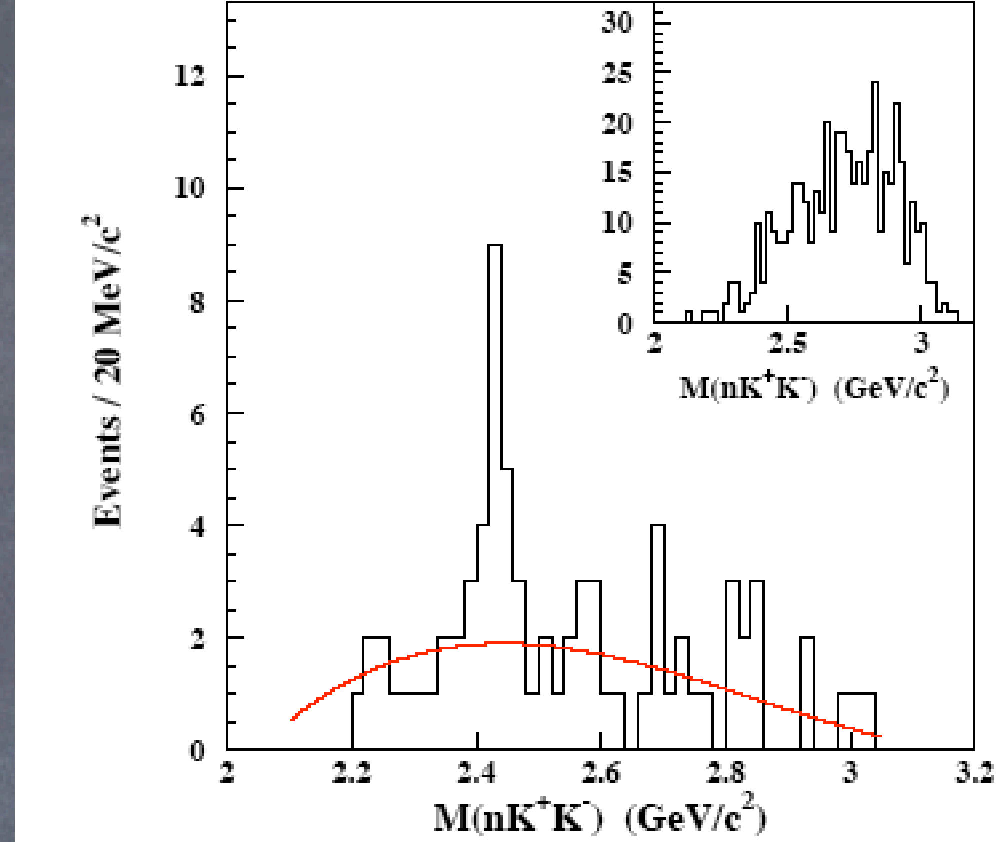

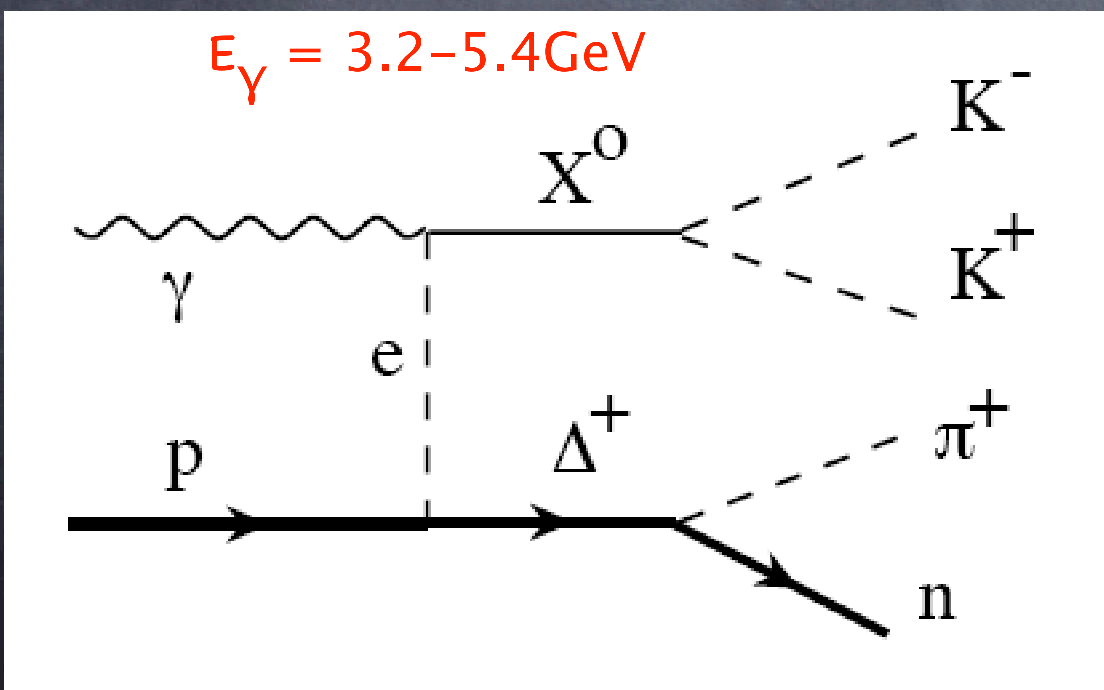

Threshold energies

$X=f_2$ W=2.51GeV

$X=a_2$ W=2.55GeV

$X=\rho_3$ W=3.31GeV

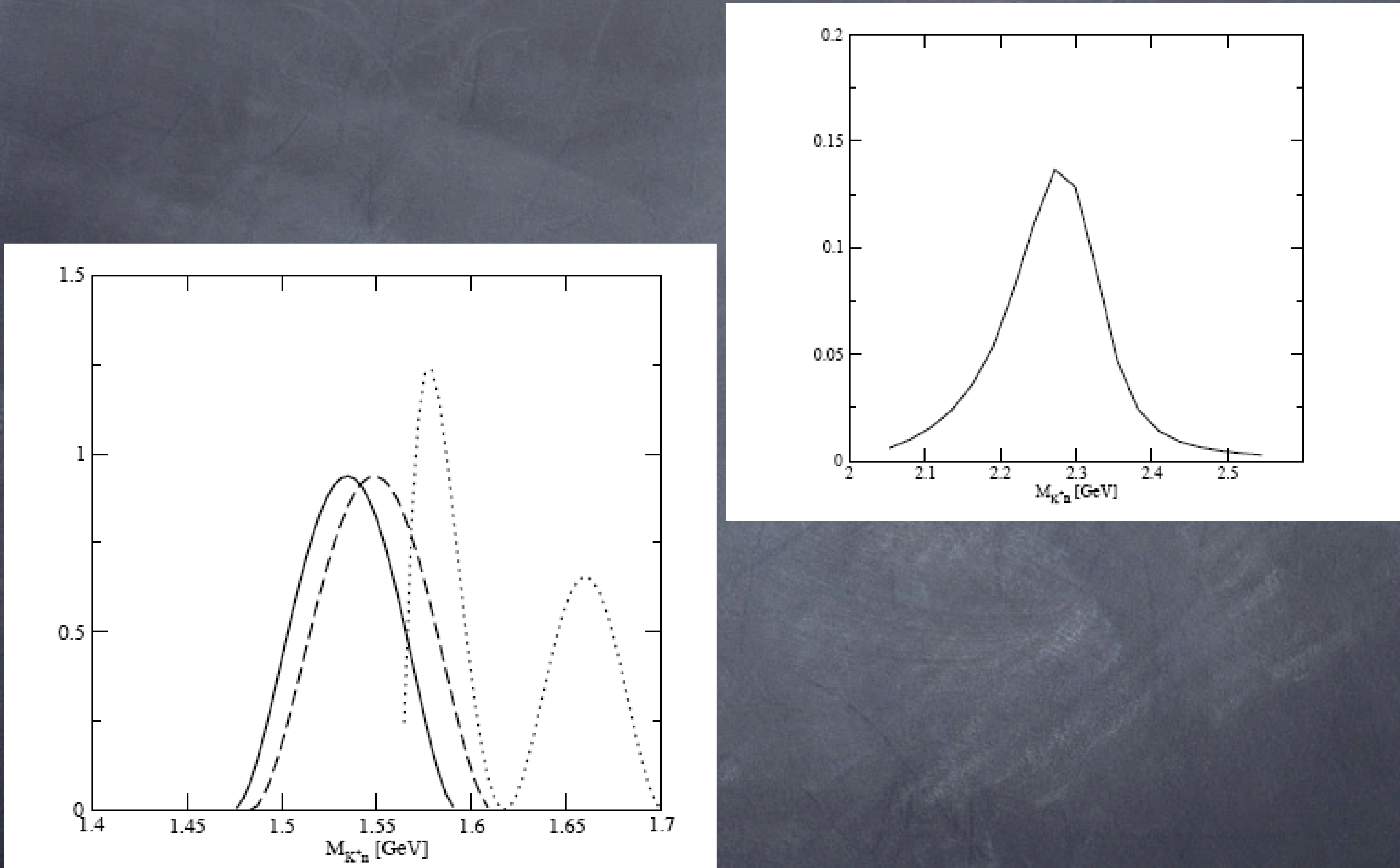

FIG. 3: The nK^+ mass distribution as described by $\int d\phi_{K^+}|Y_{J_X,\lambda_X}(\theta_{K^+n},\phi_{K^+})|^2$, for $\Delta = \Delta(1232)$ and $J_X = \lambda_X = 2$, $X = f_2$, (solid line), $J_X = \lambda_X = 2$, $X = a_2$, (dashed line), and $J_X = 3$, $\lambda_X = 1$, $X = \rho_3$ (dotted line). The $M_{nK^+K^-}$ invariant masses for the three cases are $2.22, 2.27$ and 2.64 GeV, respectively.

DIANA (ITEP, Xe bubble chamber, 850MeV K-beam)

$$K^+ Xe \rightarrow K_s^0 p X e'$$

no magnetic field

particle identified by their range in Xe

angular cut, p and Ks in the forward direction

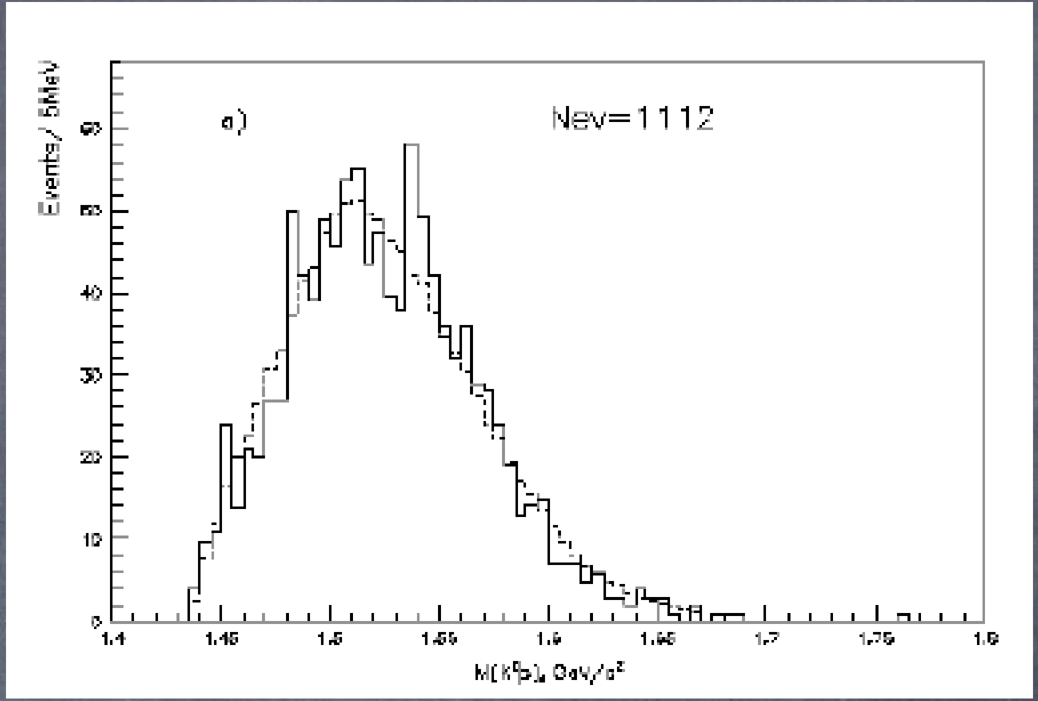

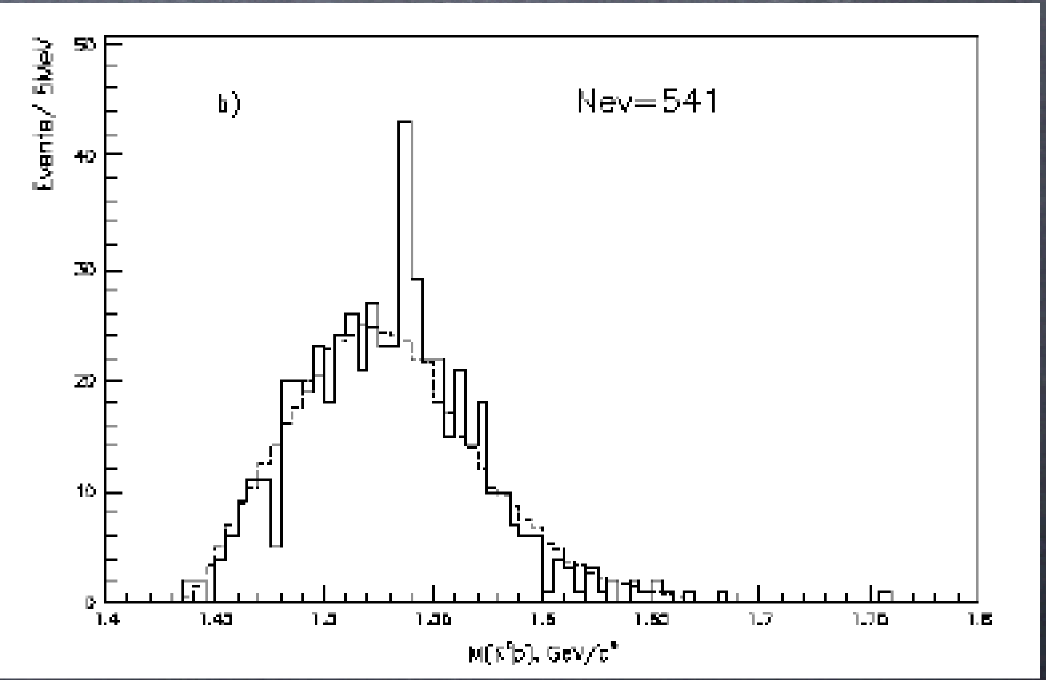

M.Zavertyaev, (hep-ph/0311250)

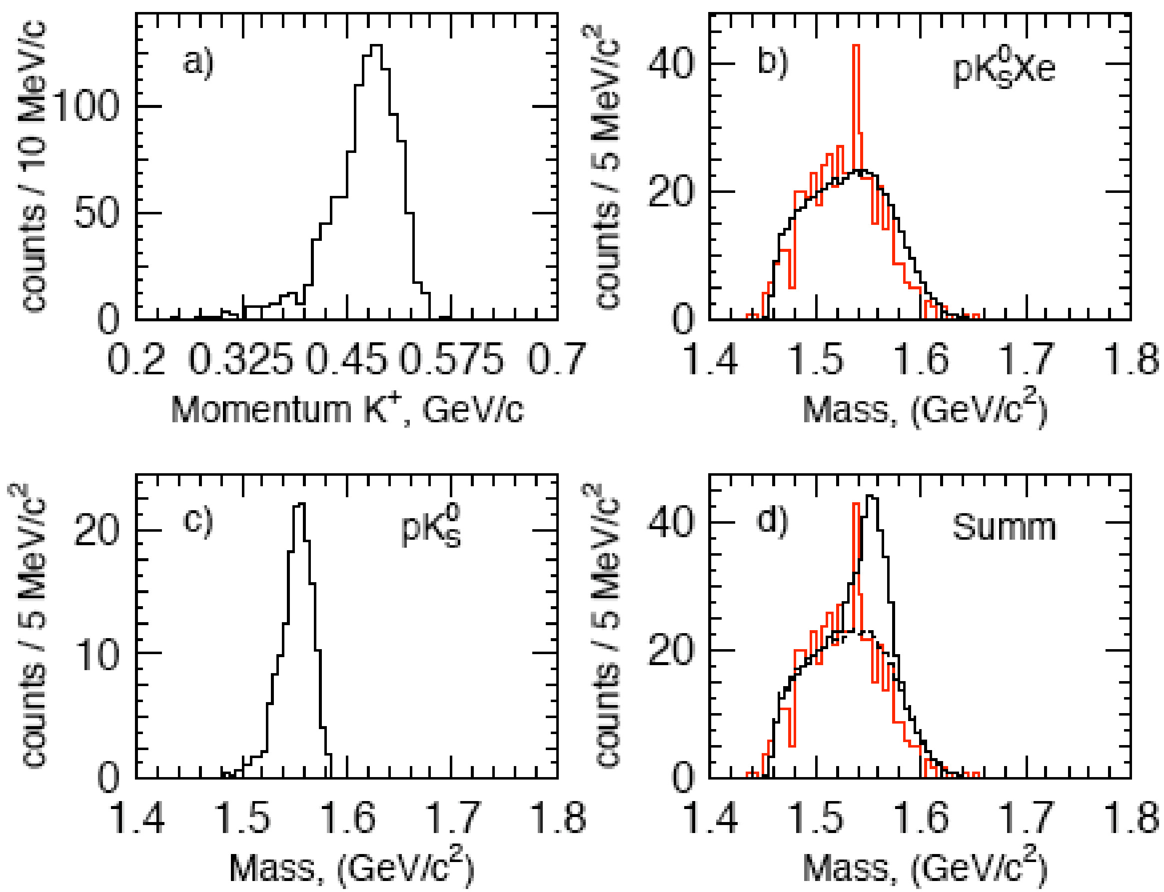

Figure 2: The experimental beam momentum [5] and MC mass spectra distribution corresponding to: b) reaction $K^+Xe \rightarrow K^0_s pXe'$; c) reaction $K^+n \rightarrow K^0_s p$; d) the summ of both b) and c); The histogram in red corresponds to the experimental mass distribution from [5].

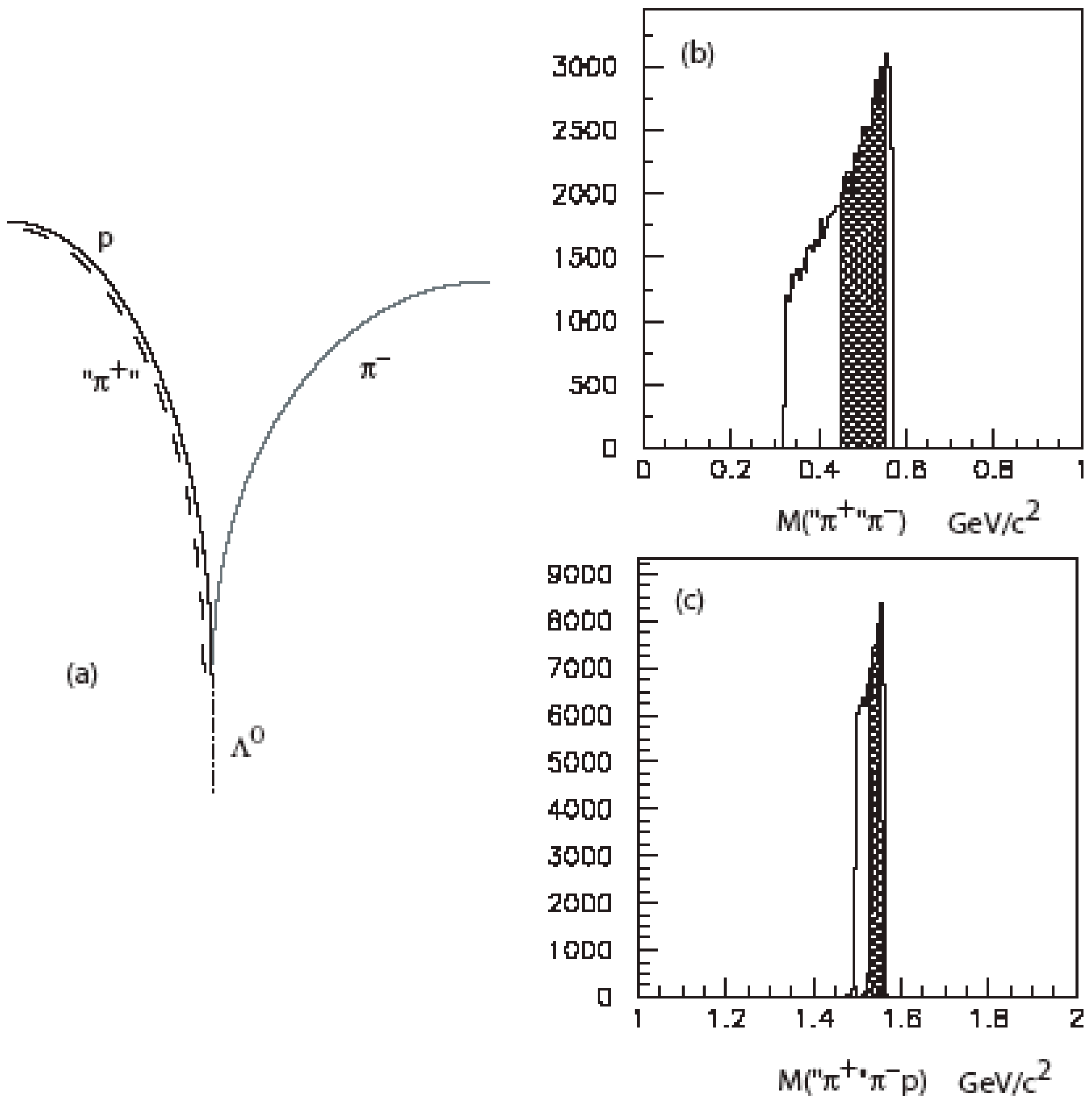

Figure 5. Figure (a) is a schematic of the decay $\Lambda^0(1115) \rightarrow \pi^- p$. The effect of spurious *ghost* tracks from the reconstruction software is considered. In this case a π^+ track is generated. When combined with the π^- from the Λ^0 the effective mass clusters about 0.5 GeV/c^2 as in Figure (b) and when the ghost track is combined with the Λ^0 decay products the effective mass clusters around 1.5 GeV/c^2 as seen in Figure (c). In the shaded distributions the $"\pi^+"\pi^-$ mass is required to be near the K^0_S. The mean of the shaded portion of the distribution in Figure (c) is 1.54 GeV/c^2, the mass of the θ^+. In this study the Λ^0 momentum in the LAB frame was uniform from 2 to 100 GeV/c.

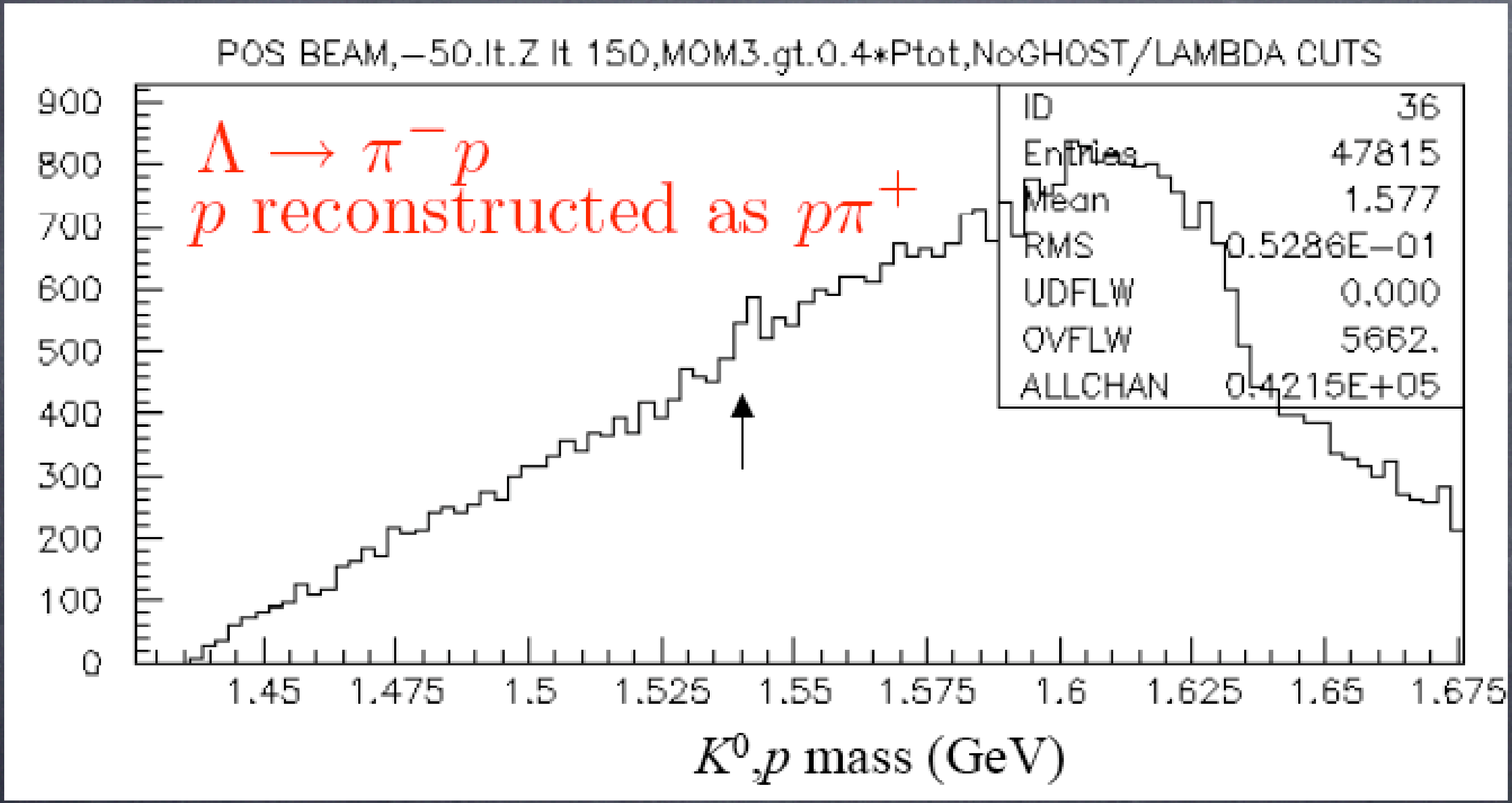

Hyper CP @ FNAL

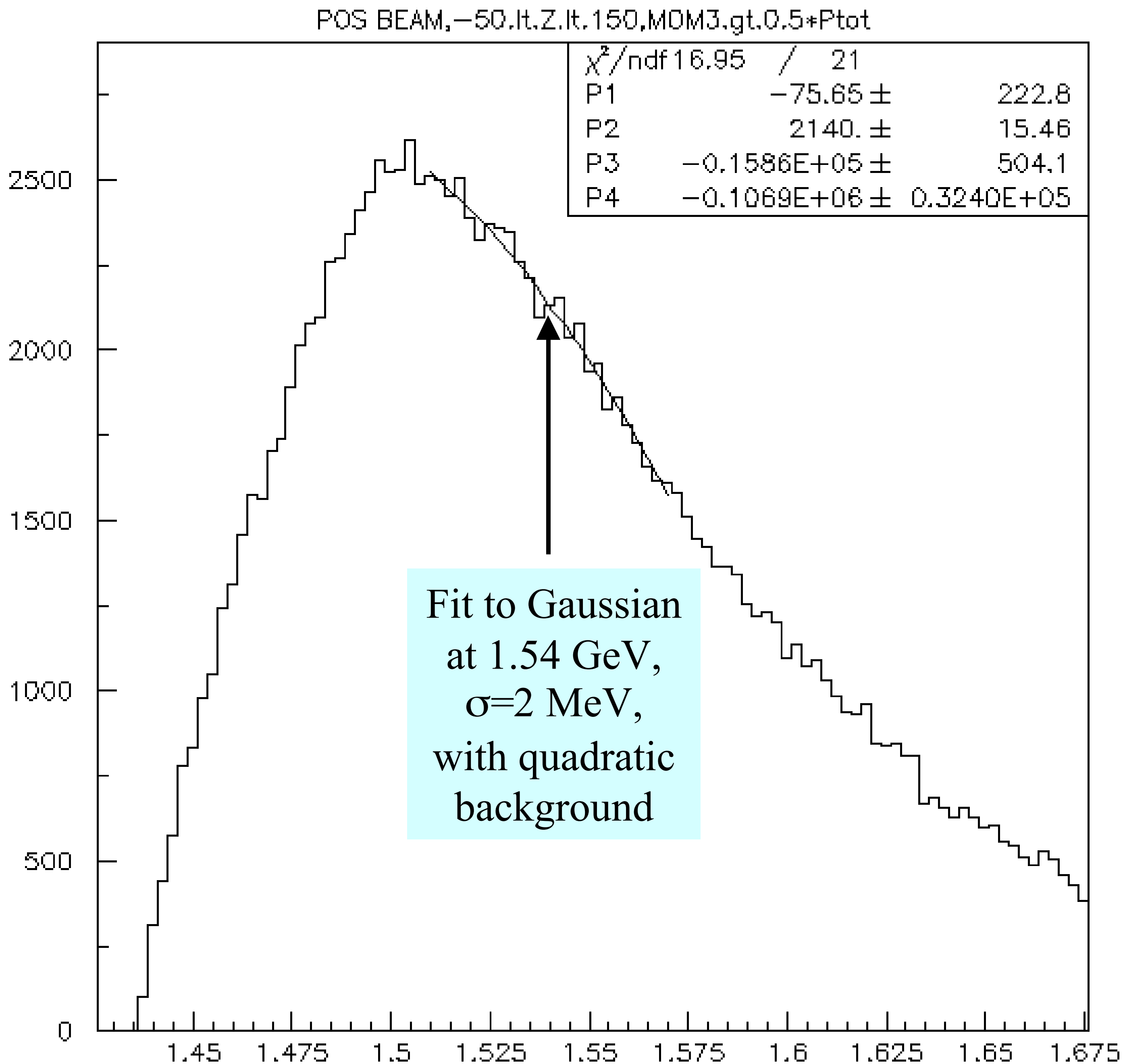

K^0-p mass, either sign

E871/HyperCP, M.Longo @ QNP04

90% CL limit ~370 events out of 150000 K^0-p candidates.

P1 is the amplitude of the gaussian.

Bins are 2 MeV

HyperCP Preliminary

Pentaquark sightings come from low statistics, low resolution, low-energy experiments with kinematically constrained final states after complicated cuts are imposed.

High resolution, high statisitcs, experiments with both low- and high- particle multiplicity do not report the pentaquarks.

3-particle Dalitz plot

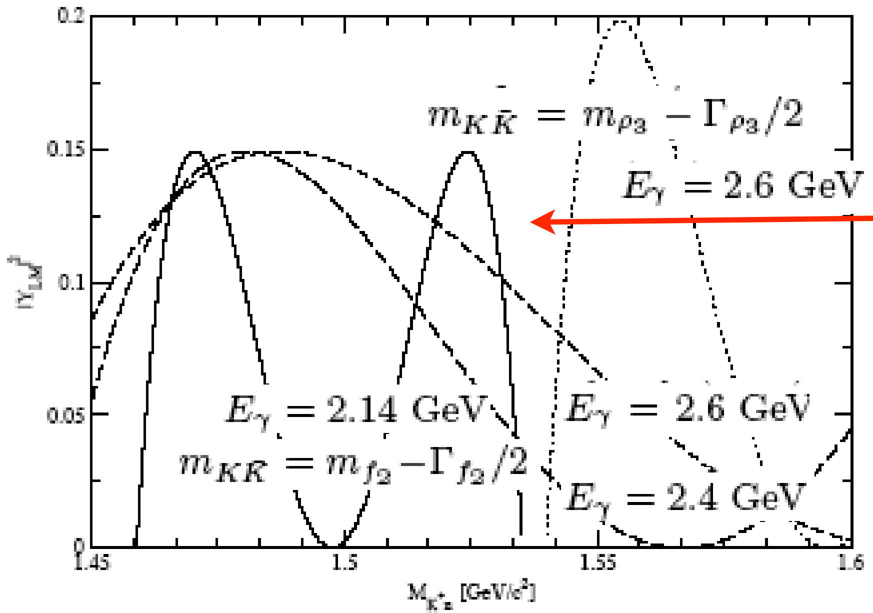

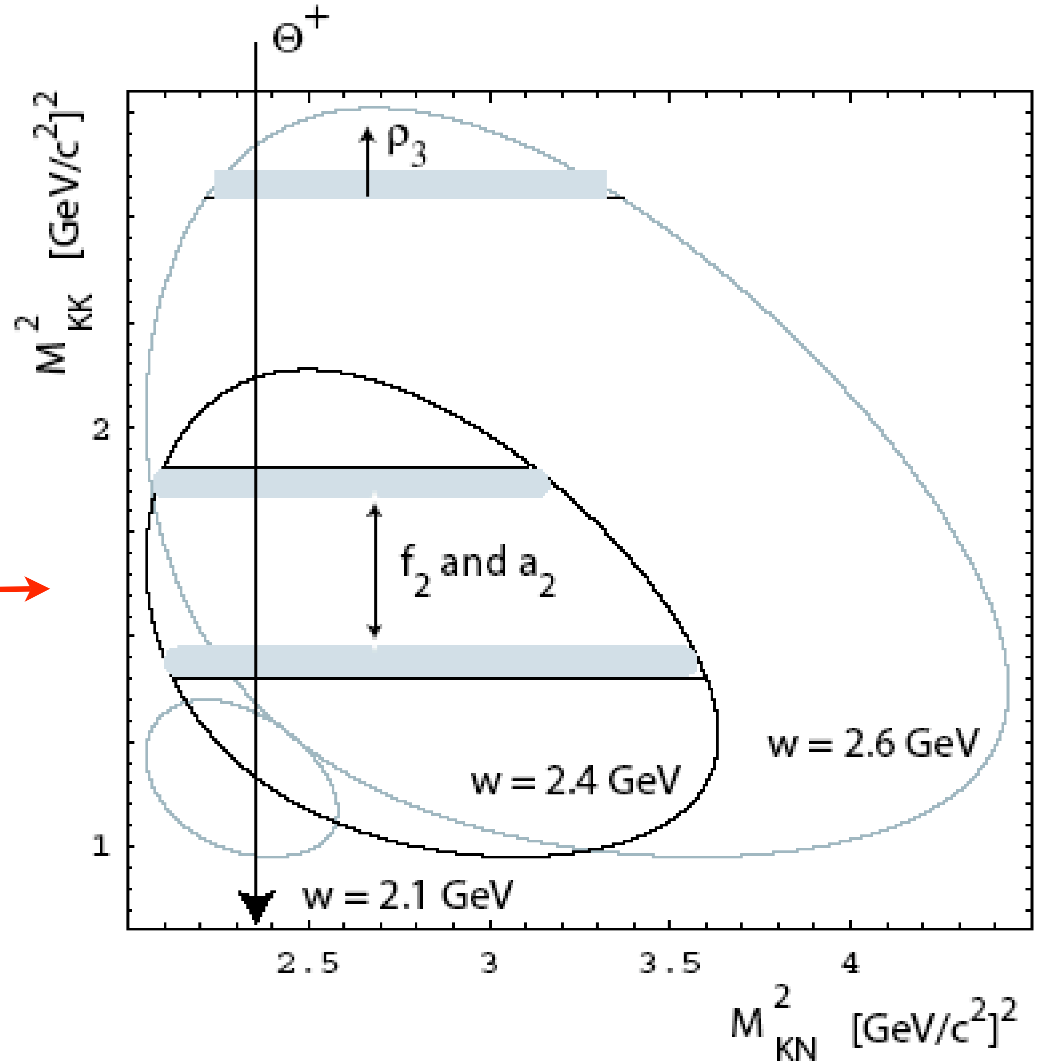

FIG. 1: Boundaries of the m^2_{KK} versus m^2_{KN} Dalitz plot for three different values of w, the energy available to the $K\bar{K}N$ system, 2.1, 2.4 and 2.6 GeV. For the data of ref. [2], the observed distribution in w rises from 2.1 GeV, peaks at 2.4 and falls to zero near 2.6 GeV. Horizontal lines denote the region spanned by the f_2 and a_2 mesons defined by their half-widths and the region of the ρ_3 starting with its central mass less its half-width. The vertical line denotes the square of the Θ mass.

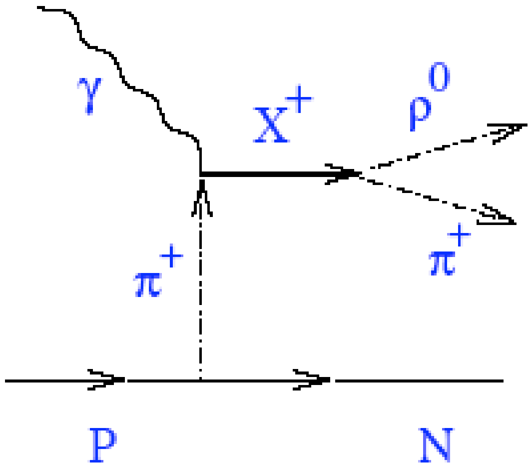

Fig. 1. $\rho^0\pi^+$ photoproduction via one-pion-exchange.

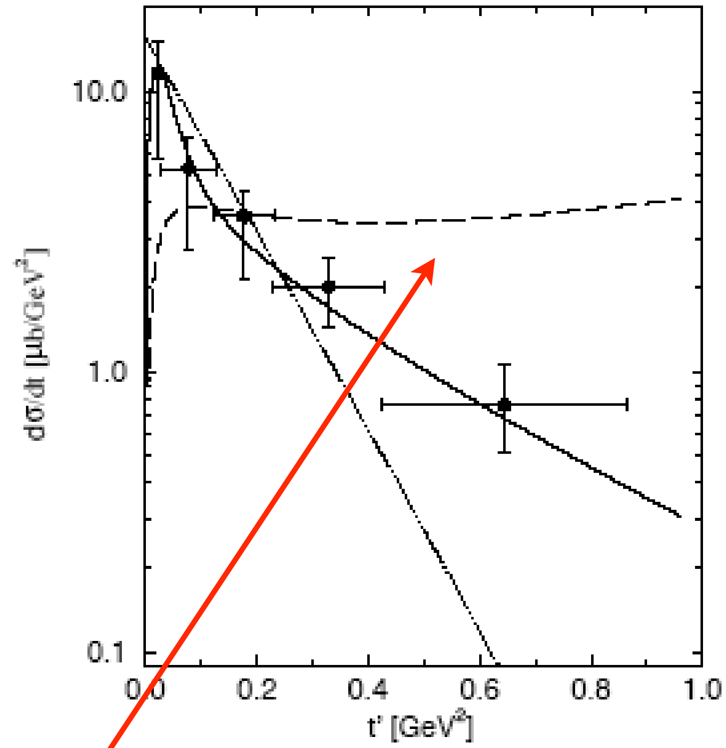

$$\frac{d\sigma}{dt}(\gamma p \to A_2{}^+ n) = \frac{\pi}{64}\,\frac{g_{\pi NN}{}^2}{4\pi}\,\frac{g_{A\pi\gamma}{}^2}{4\pi} \times \frac{1}{m_A{}^6 k^2 s}\,\frac{|t|(t-m_A{}^2)^4}{(t-\mu^2)^2},$$

Three is no known method for “fine tuning” Regge theory

Fig. 3. Momentum transfer dependence of a_2^+ photoproduction cross section. Data is from Ref. [15]. Solid line is the OPE prediction corrected to account for absorption. Dashed line is the pure OPE prediction and the dotted line is the $A\exp(-bt)$ parameterization.

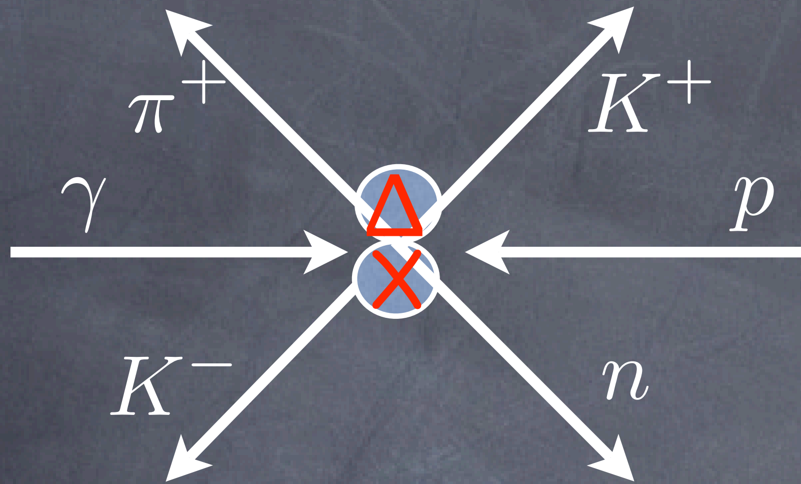

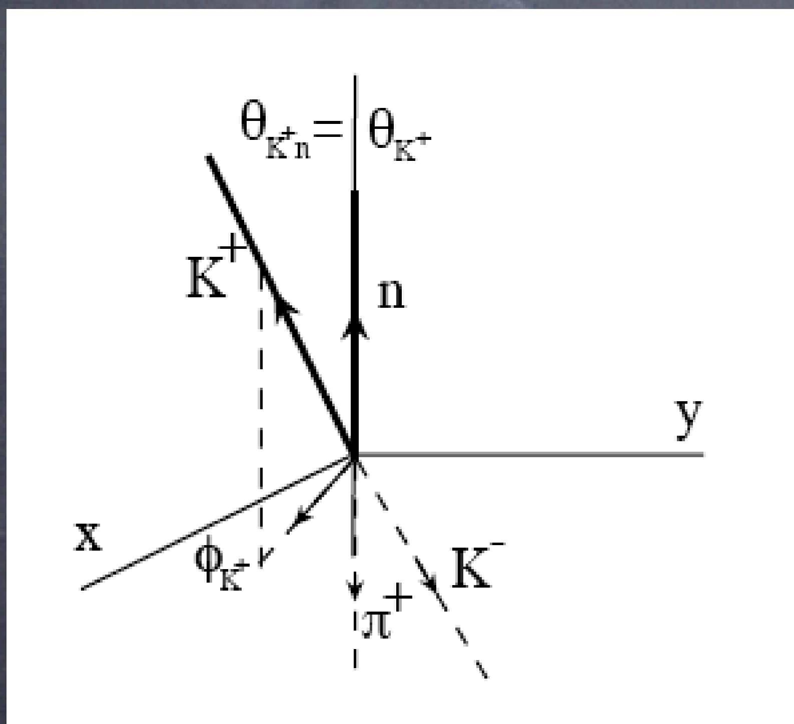

"N*" mass

$$M_{N^*} = 2.23 GeV$$

$$M_{N^*} = 2.27 GeV$$

$$M_{N^*} = 2.64 GeV$$

$$\uparrow$$

$$M_{nK^+K^-} = M_{N^*}$$

is sharp !

$$\cos\theta^*_\pi > 0.8$$

correlates n with $K^+ K^-$ helicity ->possible kinematic reflection

from $K^+ K^-$ resonance

COSY-TOF $pp \to \Sigma^+ K^0_S p$

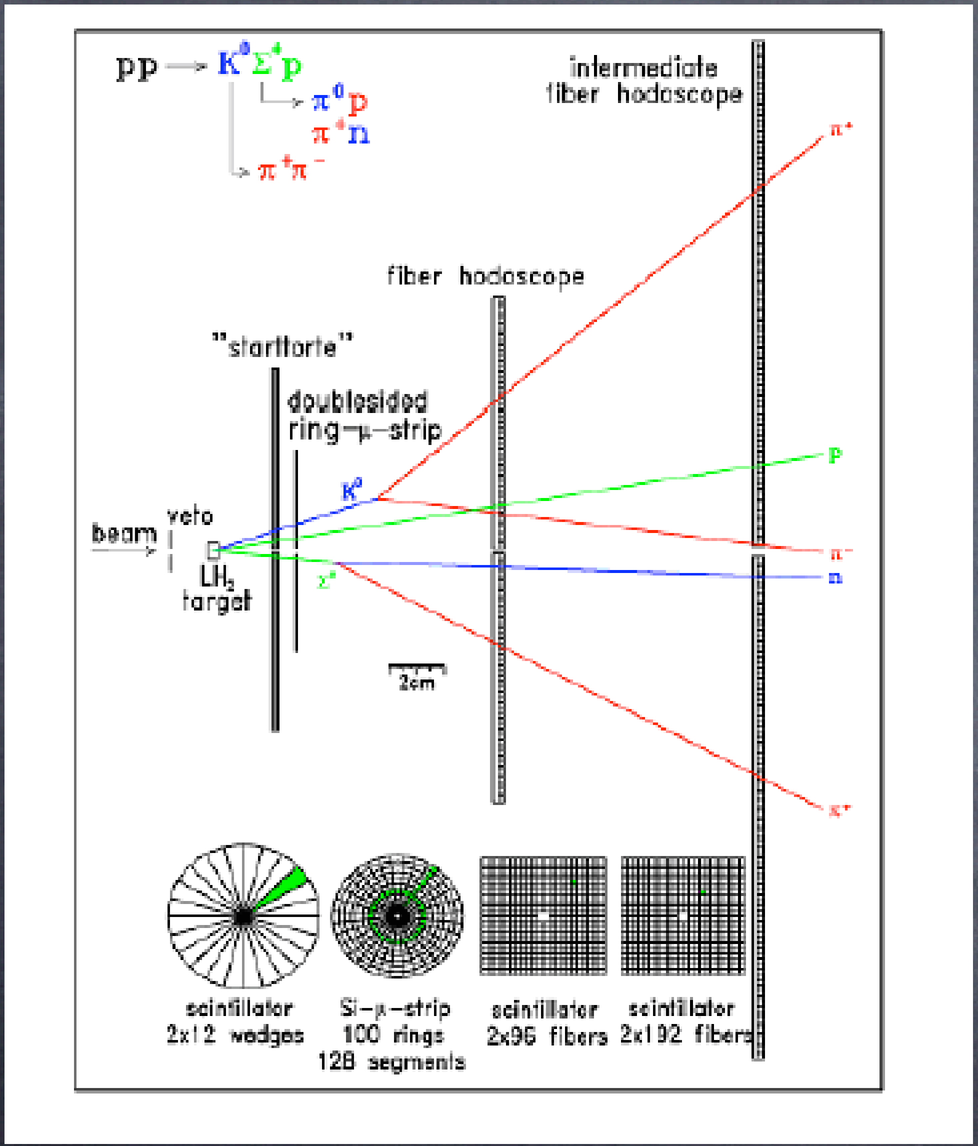

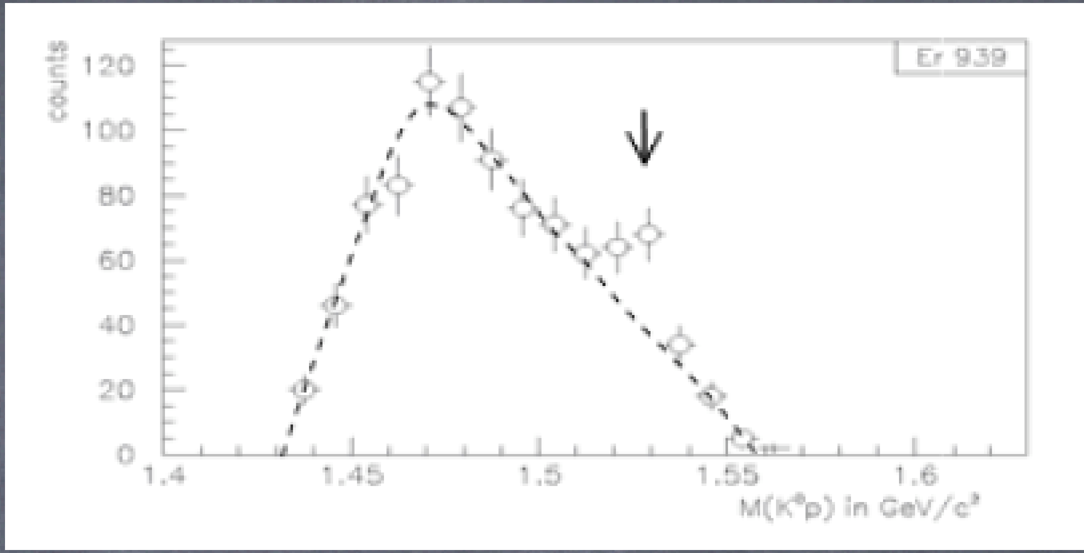

no magnetic filed, PID, pure geometry TOF no used in this analysis !